

# Impact of spatially heterogeneous residential heat pump loads on storage and generation requirements considering network constraints

Claire E. Halloran, Filiberto Fele, Malcolm D. McCulloch

*Department of Engineering Science*

*University of Oxford*

Oxford, United Kingdom

{claire.halloran, filiberto.fele, malcolm.mcculloch}@eng.ox.ac.uk

**Abstract**—This paper investigates how spatial heterogeneity in inflexible residential heat pump loads affects the need for storage and generation in the electricity system under business-as-usual and low-carbon emissions budgets. Homogeneous and heterogeneous heat pump loads are generated using population-weighted average and local temperature, respectively, assuming complete residential heat pump penetration. The results of a storage and generation optimal expansion model with network effects modeled using DC optimal power flow for a homogeneous and heterogeneous set of load profiles are compared. A case study is performed using a 3-bus network of London, Manchester, and Glasgow in Britain for load and weather data for representative weeks in 2019. Using heterogeneous heating demand data changes storage sizing: under a business-as-usual budget, 26% more total storage is built on an energy and power basis, and this storage is distributed among all of the buses in the heterogeneous case. Under a low-carbon budget, total energy storage at all buses increases 2 times on an energy basis and 40% on a power basis. The energy to power ratio of storage at each bus also increases when accounting for heterogeneity; this change suggests that storage will be needed to provide energy support in addition to power support for electric heating in high-renewable power systems. Accounting for heterogeneity also increases systems cost, particularly capital costs, due to the need for higher generation capacity in the largest load center of London and coincidence of local peak demand at different buses. These differences underscore the importance of accounting for heat pump load heterogeneity in power system planning.

**Index Terms**—component, formatting, style, styling, insert

## I. INTRODUCTION

This paper investigates how spatial heterogeneity in inflexible residential heat pump loads affects the need for storage and generation in the electricity system. The United Kingdom (UK) Climate Change Committee’s Sixth Carbon Budget identifies residential building-scale low-carbon heat as a key area for greenhouse gas emissions reduction in the buildings and foresees electrification of heating using heat pumps as the primary means for achieving this reduction [15]. Thus, heat pumps are poised to be a key decarbonization technology in the UK in the next 3 decades.

A number of studies in the last decade focus on the system effects of widespread heat pump uptake and the role of flexibility in reducing renewable curtailment and mitigating

transmission congestion [3], [5], [6]. Given the high cost and political challenges of expanding transmission lines, many of these studies focus on addressing the challenges that network constraints pose during heat pump deployment in a high-renewable system. However, these studies are fundamentally limited in their consideration of flexibility as they exclude non-heat forms of storage [6] and consider limited amounts of thermal storage [3], [5].

Heat pump deployment will change electric loads differently in different location within the same grid, depending on local temperature, housing stock, and other socio-economic factors [1], [22]. The spatial load heterogeneity that these researchers predict will impact the electricity infrastructure needed to integrate heat pumps; however, no study to date has explored the implications of heterogeneous heating demand for power system infrastructure requirements.

To understand the impact of spatial heterogeneity in heat pump load on the need for electricity infrastructure, we utilize a storage and generation expansion problem formatted as a convex optimization. This model sizes and sites new generation and storage at multiple nodes considering network effects of thermal limits on the lines between the nodes. Based on data from heat pump trials, residential heating loads are calculated using outdoor air temperature: homogeneous loads are calculated using population-weighted average temperature for the grid region, and heterogeneous loads are calculated using local temperature. This model is applied to a case study of 3 urban areas in Britain to quantify the difference in generation and storage capacity expansion required to accommodate heterogeneous heat pump load. The impact of load heterogeneity on system capital and dispatch costs is also considered.

## II. METHODOLOGY

### A. Heating demand model

To explore the effect of spatially heterogeneous heating demand on power system infrastructure requirements, we compare spatially heterogeneous heating demand, calculated based on local temperature, and spatially homogeneous heating demand, calculated based on population-weighted average

national temperature. we use a model from Watson *et al.* to generate heating demand profiles based on outdoor air temperature, assuming the heat pumps deployed are 25% ground source and 75% air source [21]. This model is chosen for its basis in real heat pump trial data and nationally representative boiler gas demand data in Britain, the geography considered in the case studies. To establish the maximum possible impact of heat pump use on the power system, we assume complete electrification of space and water heating in all households considered in the case studies.

Homogeneous heating demand is calculated using a population-weighted mean daily temperature [4], [13]. This national average daily temperature is input into the Watson *et al.* model to calculate total heating demand, which is then allocated to the areas considered in the case studies based on population. Heterogeneous heating demand for each area is calculated from the Watson *et al.* model using local mean daily temperature and the number of households in each area. The resulting heating demand has a different load profile shape and magnitude in each location.

### B. Generation and storage expansion model

A generation and storage expansion optimization problem is used to meet total demand with the lowest possible operating and capital cost. The objective of this problem is minimizing operating costs from all generator technologies  $g$  at all buses  $i$  for each time step  $t$  considered, plus the capital costs of investments in new generation capacity and storage capacity.

$$\min \sum_{g,i,t} c_{gen,g} p_{g,i}(t) + \sum_{g,i} c_{cap,g} C_{g,i}^{new} + \sum_i c_{SOC} SOC_i^{max} \quad (1)$$

where  $c_{gen,g}$  is the dispatch cost of each technology,  $c_{cap,g}$  is the new build capacity cost for each generation technology, and  $c_{SOC}$  is the cost of energy storage capacity. The decision variables are:  $p_{g,i}(t)$ , the power generated by each technology at each bus at each time,  $C_{g,i}^{new}$ , the new generation capacity build of each technology at each bus, and  $SOC_i^{max}$ , the maximum state of charge (also known as energy capacity) for the storage unit at each bus. The capital costs are divided quarterly over the expected lifetime of the assets since only 12 representative weeks are considered.

This objective function is subject to the constraints in (2)-(15). Unless otherwise noted, these equations apply for all buses  $i$  in the set of buses  $\mathcal{I}$ , all times  $t$  in the set of time steps in the time period considered  $\mathcal{T}$ , and for all generation technologies  $g$  in the set of modeled generation technologies  $\mathcal{G}$ . Equation (2) shows the bus-network power balance constraint.  $L_{il}$  is the bus-line matrix, which is equal to 1 if line  $l$  originates at bus  $i$ , -1 if line  $l$  terminates at bus  $i$ , and 0 otherwise. Positive flow  $p_{line+,l}$  corresponds to flow in the same direction of the line, while negative flow  $p_{line-,l}$  is in the opposite direction listed in the bus-line matrix.  $\mathcal{L}_i$  is the set of lines connected to bus  $i$ . The DC power flow approximation is (3):  $B_{ij}$  is the matrix of the reactance of the line between buses  $i$  and  $j$  and  $\delta_i$  is the

voltage angle at bus  $i$ . Equation (4) describes the thermal line limits, where  $\mathcal{L}$  is the set of all lines in the network. Generation limits based on the availability of each generation technology are shown in (5) for the set of modeled generation technologies  $\mathcal{G}$ . The availability factor  $A_{g,i}$  is a value between 0 and 1 that represents the location-specific availability of each generation technology. The availability factor for non-renewables generation technologies is always 1. The existing generation capacities are represented as  $C_{g,i}^{old}$ . Equation (6) reflects the carbon budget limit on fossil fueled generator use, with  $\epsilon_g$  as the carbon emissions intensity of generating a unit of energy from technology  $g$ ,  $\tau$  the length of time interval  $t$ , and  $E_{lim}$  the emission limit set for time period  $\mathcal{T}$ .

$$p_{net,i}(t) = \sum_l L_{il} (p_{line+,l}(t) - p_{line-,l}(t)) \quad \forall l \in \mathcal{L}_i \quad (2)$$

$$p_{line+,l}(t) - p_{line-,l}(t) = B_{ij}(\delta_i - \delta_j) \quad \forall i, j \text{ connected by line } l \quad (3)$$

$$-p_l^{max} \leq p_{line+,l}(t) - p_{line-,l}(t) \leq p_l^{max} \quad \forall l \in \mathcal{L} \quad (4)$$

$$0 \leq p_{g,i}(t) \leq A_{g,i}(t)(C_{g,i}^{old} + C_{g,i}^{new}) \quad (5)$$

$$\sum_{g,i,t} \tau \epsilon_g p_{g,i}(t) \leq E_{lim} \quad (6)$$

Equation (7) enforces the bus-generator power balance, where  $p_{g2n,i}$  is the power from the generators injected into the network,  $p_{g2d,i}$  is the power from the generators used to meet load, and  $p_{g2s,i}$  is the power from the generators stored in local storage. Equation (8) gives the net power balance at each bus, where  $\eta$  is the storage discharge efficiency,  $p_{n2s,i}$  is the power from the network stored at bus  $i$ , and  $p_{n2d,i}$  is the power from the network used to meet load at bus  $i$ . Demand-supply balance is guaranteed by (9), where  $p_{d,i}$  is the demand at each bus  $i$ ,  $p_{g2d,i}$  is the power from generation at bus  $i$  used to meet demand at the same bus, and  $p_{s2d,i}$  is the power from storage used to meet demand at the same bus  $i$ .

$$\sum_g p_{g,i}(t) = p_{g2n,i}(t) + p_{g2d,i}(t) + p_{g2s,i}(t) \quad (7)$$

$$p_{net,i}(t) = p_{g2n,i}(t) + \eta p_{s2n,i}(t) - p_{n2s,i}(t) - p_{n2d,i}(t) \quad (8)$$

$$p_{d,i}(t) = p_{g2d,i}(t) + \eta p_{s2d,i}(t) + p_{n2d,i}(t) \quad (9)$$

Equations (10) through (16) constrain the storage units. Equations (10) and (11) give the storage charging and discharging power limits, respectively, with  $p_{s,i}^{max}$  as the maximum storage power capacity. The state of charge of each storage unit is limited in (12), where  $SOC_i$  is the state of charge of the storage unit at bus  $i$ . This is the state of charge from the previous time step plus the sum of power flows into and out of the storage unit at the previous time step, times the length of the time steps, as shown in (13). In the first time period considered, the state of charge is defined by the decision variable  $SOC_{i,0}$  (see (14)). Equation (15) enforces state of charge periodicity. Equation (16) limits the ratio of storage energy capacity to power capacity to be between 1 and 4 hours,

in line with typical values for grid-scale lithium-ion storage facilities.

$$0 \leq p_{g2s,i}(t) + p_{n2s,i}(t) \leq p_{s,i}^{max} \quad (10)$$

$$0 \leq p_{s2n,i}(t) + p_{s2d,i}(t) \leq p_{s,i}^{max} \quad (11)$$

$$0 \leq SOC_i(t) \leq SOC_i^{max} \quad (12)$$

$$SOC_i(t) = SOC_i(t-1) + p_{n2s,i}(t-1)\tau + p_{s2n,i}(t-1)\tau - p_{s2d,i}(t-1)\tau \quad \forall t \in \mathcal{T}, t \neq 0 \quad (13)$$

$$SOC_i(t=0) = SOC_{i,0} \quad (14)$$

$$SOC_i(t=final) = SOC_{i,0} \quad (15)$$

$$1 \leq SOC_i^{max}/p_{s,i}^{max} \leq 4 \quad (16)$$

### C. Case study: 3-bus Britain model

We consider a case study of 3-bus system in which each bus corresponds to an urban area in Britain: greater Glasgow, the Manchester built-up-area, and the London built-up-area. These urban areas were selected for their large populations as well as their large geographic distance from one another.

Weather and electric demand data from representative weeks in 2019 are used. Non-heating electric demand data for each urban area was approximated by dividing the historical demand profile by the proportion of the population residing in each urban area [10], [14], [19]. This base demand was added to the heating demand profiles.

Renewable potential profiles for different locations were generated based on historical weather data using the renewables.ninja tool [12]. For offshore wind potentials, historical weather data was taken from the location of the nearest offshore wind farm built by the end of 2018 (London Array for London, Walney for Manchester, and Beatrice for Glasgow). Because most load is often within urban areas and most generation is outside of urban areas, the renewable and conventional generation capacity of the entire NUTS 1 region<sup>1</sup> at the end of 2018 was allocated to the corresponding urban area [17], [18]. All conventional generation capacity is modeled as combined cycle gas turbines (CCGT). The London region has relatively little generation capacity, so half the capacity of South East England is assumed to be used to meet the electricity demand of the London built-up area.

Nuclear generation and interconnector imports are fixed at their historical levels for 2019 [2]. Grid-wide nuclear dispatch is allocated to each bus in proportion to the nuclear capacity in each region and priced at its marginal operation price of \$29,000 per GWh [7]. Interconnector imports are allocated to the nearest bus considered in the case study and priced at \$11,000 per GWh, based on typical 2019 auction prices [11]. Nuclear and interconnector capacity expansion are not considered in this case study.

<sup>1</sup>Nomenclature of Territorial Units for Statistics. NUTS 1 defines regional level subdivision of the UK territory

Representative weeks were selected for each month to capture low-wind, low-temperature extremes. Heinen *et al.* identified these weather conditions as critical situations in systems with electrified heating and large wind generation in the context of Ireland [6]. Thus, for each month, minimum net demand hour is identified. Net demand is defined as the difference between total heterogeneous demand and total wind generation based on 2018 wind capacity. The sample week was the 4 days prior to the day on which this minimum net demand hour occurred and the following 3 days. This process results in a set of 12 sample weeks of weather and demand conditions that represent system extremes throughout the year. Capturing these extremes is crucial for ensuring that adequate capacity is built.

Levelized cost of energy values for 2019 were used for the dispatch prices of all generation technologies, and dispatch from storage was assumed to have no cost [7]. Capital costs for generation technologies were determined using quarterly nameplate capacity costs for new generation built in 2019 [7]. For storage, 2019 nameplate energy capacity cost for lithium-ion batteries was used [8]. To minimize unused storage power capacity, an arbitrarily small price of \$10 per GW was assigned. A storage efficiency of 90% is assumed.

Transmission lines were assumed to connect all cities to one another. Line reactance values were calculated using the distance between cities and a per length reactance value of 0.019 % p.u. per km, which is in line with the reactance values for high-voltage transmission lines in the Great Britain system [9]. Transmission capacity between each bus was assumed to be 5 GW.

This case study was performed with two different carbon budgets based on the UK Climate Change Committee's (CCC) Sixth Carbon Budget for electricity generation [16]: a 2019 budget reflecting business-as-usual emissions and a 2035 budget reflecting aggressive decarbonization. Because the urban areas included represent about one-fifth of the total UK population and the high-demand winter period is considered, 10% of the CCC carbon budget is used for this case study. A carbon intensity of 365 g CO<sub>2</sub>e per kWh [20] is assumed for CCGT generation. All other generation is considered carbon-free.

## III. RESULTS AND DISCUSSION

### A. Homogeneous and heterogeneous heat demand

In the case study considered, using a single grid-wide temperature to generate homogeneous demand profiles did not fully capture the high heat demand periods at each bus that are present in the heterogeneous demand profiles. Regardless of the heating profile used, this model suggests that switching to heat pumps for domestic space and water heating will drastically increase electric demand in urban areas. However, using a local temperature-based model leads to much higher peak and average demand: for instance, considering homogeneous heating demand about doubles the historical average demand in London to 11 GW and heterogeneous demand further increases average demand to 13 GW. Peak demand

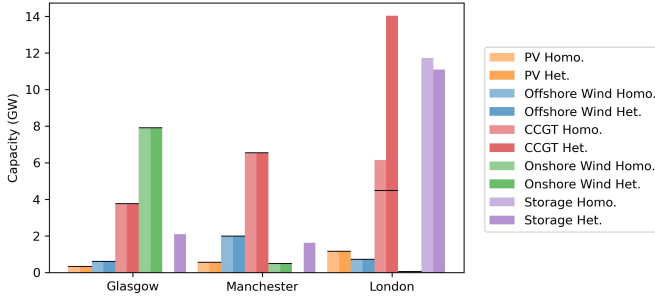


Fig. 1. Capacity expansion for homogeneous and heterogeneous heating demand under 2019 carbon budget, with existing generation capacity in 2018 indicated by the black line.

for the London urban area also increases from 22 GW in the homogeneous case to 30 GW in the heterogeneous case. The homogeneous demand profile based on national population-weighted average temperature data, including warmer coastal areas in the south, lacks the peaks and valleys in heating demand that are clear in the heterogeneous profiles of these inland cities. For the winter peak demand period considered, the differences in demand can be relatively large, and capturing these extreme grid conditions is crucial for power system planning.

### B. 3-bus Britain model

1) *2019 Carbon Budget*: Figure 1 shows the added capacity of different technologies at each bus to meet electric heating demand for a 2019 carbon budget. Storage capacity is added at all buses to meet heterogeneous heating demand, but the storage capacity at the London bus is slightly decreased for heterogeneous demand. Only the London bus adds any generation capacity, all of which is CCGT, to meet both homogeneous and heterogeneous demand. Because transmission constraints limit power imports from other buses, the London bus requires additional generation to meet its large peak demand. Added CCGT capacity increases dramatically from 1.7 GW in the homogeneous case to 9.6 GW in the heterogeneous case. This fivefold increase is much larger than the 34% increase in peak demand between the two cases because in the heterogeneous case high demand in London coincides with high demand in Manchester on the maximum CCGT use day. This coincidence necessitates more local CCGT capacity in London to meet demand since imports from other buses cannot be relied upon.

More detail about the optimal storage energy and power capacity under a 2019 carbon budget is shown in Table I. Storage is only deployed at the London bus in the homogeneous demand case, but is distributed among all buses in the heterogeneous demand case. The total storage deployed also slightly increases from 11.7 GW/11.7 GW h to 14.8 GW/14.8 GW h. Storage power and energy capacity at the London bus slightly decreases from 11.7 GW in the homogeneous case to 10.9 GW in the heterogeneous case because the CCGT capacity added at the bus can partially substitute for storage.

TABLE I  
STORAGE SIZE

	Max. SOC (GWh)	Max. Power (GW)
<i>2019 carbon budget</i>		
Homo. heating (total)	11.7	11.7
Glasgow	0.00	0.00
Manchester	0.00	0.00
London	11.7	11.7
Het. heating (total)	14.8	14.8
Glasgow	2.09	2.09
Manchester	1.62	1.62
London	11.1	11.1
<i>2035 carbon budget</i>		
Homo. heating (total)	14.2	7.94
Glasgow	0.00	0.00
Manchester	0.00	0.00
London	14.2	7.94
Het. heating (total)	32.8	11.6
Glasgow	0.00	0.00
Manchester	0.45	0.45
London	32.3	11.1

TABLE II  
SYSTEM COSTS

	Capital cost (\$B)	Dispatch cost(\$B)
<i>2019 carbon budget</i>		
Homo. heating	0.27	1.04
Het. heating	0.65	1.29
<i>2035 carbon budget</i>		
Homo. heating	1.26	0.98
Het. heating	3.62	1.13

The impact of considering heating demand heterogeneity on estimated systems costs can be observed in Table II, which shows the quarterly capital and dispatch costs under the 2019 carbon budget. Heterogeneous heating load results in a 2.4 times higher capital cost than homogeneous demand. This difference is primarily driven by the higher CCGT capacity deployed at the London bus and increase in total storage capacity. A much smaller difference is observed in the dispatch cost for the two load scenarios: meeting heterogeneous load is 14% more expensive than meeting homogeneous heating demand, mostly due to the additional energy needed to supply higher average demand.

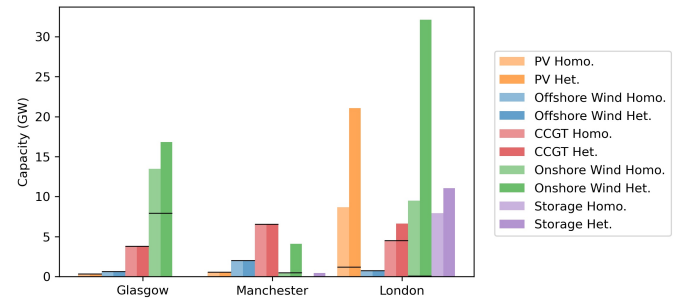


Fig. 2. Capacity expansion for homogeneous and heterogeneous heating demand under 2035 carbon budget, with existing generation capacity in 2018 indicated by the black line.

2) *2035 Carbon Budget*: Fig. 2 shows capacity expansion at each bus considering homogeneous and heterogeneous heating demand under the 2035 carbon budget. In the heterogeneous case, additional onshore wind is added at all buses to compensate for the limit on CCGT generation and storage is added at the London and Manchester buses.

As in the 2019 carbon budget, higher peak load under the heterogeneous scenario in combination with transmission constraints drives drastic generation expansion in London. Due to the strict carbon budget in 2035, the majority of this capacity is onshore wind and photovoltaic (PV), though some additional CCGT is built. Onshore wind capacity in London over triples from 9 GW in the homogeneous case to 32 GW in the heterogeneous case. PV capacity increases by 2.7 times from 7.5 GW in the homogeneous case to 19.9 GW in the heterogeneous case.

Table I shows the maximum state of charge and maximum power capacity of the storage units added under the 2035 carbon budget. Compared to the 2019 carbon budget scenario, more total storage energy capacity but less total storage power capacity is deployed under the 2035 carbon budget. This increase in the total energy-to-power ratio suggests that storage is used to provide energy for longer periods of time than under the 2019 budget, probably due to partial substitution for constrained CCGT flexible generation.

Large differences between storage expansion in the homogeneous and heterogeneous case are notable. Storage energy capacity increases by 2.3 times in the heterogeneous heating scenario compared to the homogeneous case. The bulk of this energy capacity is added at the London bus to increase utilization of power from the larger onshore wind and PV capacity in the heterogeneous case. These results suggest failing to account for spatial heat pump load heterogeneity may lead to substantial underestimation of flexibility requirements for integrating heat pumps into a renewable-dominated electric system.

Table II reveals a similar comparison between homogeneous and heterogeneous heating demand as for the 2019 carbon budget. Quarterly capital costs are 2.9 times higher to meet heterogeneous heating load compared to homogeneous heating load. This difference is primarily driven by the large increase in onshore wind capacity in London. Dispatch costs are 15% higher for the heterogeneous case; this difference reflects the cost of meeting greater total energy demand.

Quarterly capital costs for the same heating scenario are 4.6 and 5.6 times higher for the 2035 carbon budget than the 2019 carbon budget (for the homogeneous and heterogeneous scenario respectively). This cost increase reflects the cost of building oversized intermittent renewable generation to decrease the use of CCGT generation during low-wind periods.

#### IV. CONCLUSION

This paper explored the effect of spatial heterogeneity in residential electricity demand under 100% heat pump penetration on system generation and storage requirements. Overall, we find that accounting for heterogeneity in heating

demand leads to differences in storage allocation, generation expansion, and system costs. In the case study considered, using a local temperature-based, heterogeneous heating demand model leads to much higher peak and average demand, which changes generation and storage capacity requirements. Because of transmission constraints, more generation capacity is needed to meet higher peak demand in London, the largest load center. Coincident peaks in heterogeneous demand at different buses further increase capacity needs compared to the case with nationally homogeneous heating demand. These differences leads to much higher capital costs, and the discrepancy between capital costs using homogeneous and heterogeneous load is even more pronounced under a strict carbon budget. These results suggest that failing to account for spatial heat pump load heterogeneity may lead to substantial underestimation of flexibility requirements and system costs for heat pumps integration in a renewable-dominated electric system. Overall, these findings demonstrate the importance of considering heterogeneity in electric heating load for power system planning studies.

#### REFERENCES

- [1] Sven Eggimann, Jim W. Hall, and Nick Eyre. A high-resolution spatio-temporal energy demand simulation to explore the potential of heating demand side management with large-scale heat pump diffusion. *Applied Energy*, 236(June 2018):997–1010, 2019.
- [2] Exelon. Historic generation by fuel type, 2019.
- [3] Ankita Gaur, Desta Fitiwi, and John Curtis. Deep electrification of residential heating and possible implications: An Irish perspective. In *2020 5th International Conference on Advances on Clean Energy Research (ICACER 2020)*, volume 173, 2020.
- [4] Global Modeling and Assimilation Office (GMAO). MERRA 2D IAU Diagnostic, Single Level Meteorology, Time Average 1-hourly V5.2.0 (MATINXSLV), 2008.
- [5] Andrej Guminski, Felix Böing, Alexander Murmann, and Serafin von Roon. System effects of high demand-side electrification rates: A scenario analysis for Germany in 2030. *Wiley Interdisciplinary Reviews: Energy and Environment*, 8(2):1–12, 2019.
- [6] Steve Heinen, William Turner, Lucy Cradden, Frank McDermott, and Mark O'Malley. Electrification of residential space heating considering coincidental weather events and building thermal inertia: A system-wide planning analysis. *Energy*, 127:136–154, 2017.
- [7] Lazard. Levelized Cost of Energy Analysis. Technical report, 2019.
- [8] Lazard. Levelized Cost of Storage Analysis. Technical report, 2019.
- [9] National Grid ESO. Electricity Ten Year Statement - Appendix B - System technical data, 2020.
- [10] National Grid ESO. GB Historic Demand Data 2019, 2020.
- [11] Joint Allocation Office. European electricity market auction results, 2019.
- [12] Stefan Pfenninger and Iain Staffell. Long-term patterns of European PV output using 30 years of validated hourly reanalysis and satellite data. *Energy*, 114:1251–1265, 2016.
- [13] S. Reis, T. Liska, S. Steinle, E. Carnell, D. Leaver, E. Roberts, M. Vieno, R. Beck, and U. Dragosits. UK gridded population 2011 based on Census 2011 and Land Cover Map 2015, 2017.
- [14] Scotland's Census. Greater Glasgow (Settlement 2010) Usual Resident Population, 2011.
- [15] UK Climate Change Committee. The Sixth Carbon Budget: Buildings. Technical report, 2020.
- [16] UK Climate Change Committee. The Sixth Carbon Budget: Electricity generation. Technical report, 2020.
- [17] UK Department for Business Energy and Industrial Strategy. Digest of UK Energy Statistics (DUKES): electricity, 2020.
- [18] UK Department for Business Energy and Industrial Strategy. Regional Renewable Statistics: Renewable electricity by local authority, 2014 to 2019, 2020.

- [19] UK Office for National Statistics. 2011 Census: Characteristics of Built-Up Areas. Technical report, 2013.
- [20] UK Parliamentary Office of Science and Technology. Carbon Footprint of Electricity Generation. Technical report, Houses of Parliament, 2011.
- [21] S. D. Watson, K. J. Lomas, and R. A. Buswell. How will heat pumps alter national half-hourly heat demands? Empirical modelling based on GB field trials. *Energy and Buildings*, 238:110777, 2021.
- [22] Philip R. White, Joshua D. Rhodes, Eric J.H. Wilson, and Michael E. Webber. Quantifying the impact of residential space heating electrification on the Texas electric grid. *Applied Energy*, 298(January):117113, 2021.